DOI 10.1515/gps-2013-0059 — Green Process Synth 2013; 2: 381–395

Simon Schulze*, Bruno Cortese, Matthias Rupp, Mart H.J.M. de Croon, Volker Hessel, Julien Couet, Jürgen Lang and Elias Klemm

Investigations on the anionic polymerization of butadiene in capillaries by kinetic measurements and reactor simulation

Abstract: For the first time the anionic polymerization of 1,3-butadiene (Bd) is successfully transferred from semi-batch into a continuous microfluidic setup with comparable product properties. The molecular weight distribution described by the polydispersity index (PDI) is commonly used as a key criterion for product quality. The steady state and the local resolution of a continuous setup provide the opportunity to investigate the progress of the PDI during anionic polymerization. In this work, the influence of kinetics (statistics) and fluid dynamics (FD) on the PDI of the product is investigated. Therefore a dedicated setup was designed and erected to keep Bd in the liquid phase and provide a pulsation free constant liquid flow. With optimized parameter settings, a separation of initiation and propagation is obtained and the intrinsic kinetics of propagation are determined. To explain the experimental results, an ideal plug flow and an ideal laminar flow model are applied and compared to computational fluid dynamics (CFD) simulations. Finally, it is concluded which FD and statistical contributions lead to the very low PDI of 1.04 found in the experiments.

Keywords: 1,3-butadiene; intrinsic kinetics; living anionic; microreactor; polydispersity; polymerization; process intensification.

***Corresponding author: Simon Schulze,** Institute of Chemical Technology, University of Stuttgart, Pfaffenwaldring 55, 70569 Stuttgart, Germany, e-mail: simonschulze@yahoo.de
Matthias Rupp and Elias Klemm: Institute of Chemical Technology, University of Stuttgart, Germany
Bruno Cortese, Mart H.J.M. de Croon and Volker Hessel: Dept. of Chem. Engineering and Chemistry, TU Eindhoven, 5600 MB Eindhoven, Netherlands
Julien Couet and Jürgen Lang: Evonik Industries AG, Rellinghauser, Straße 1-11, 45128 Essen, Germany

1 Introduction

Within the framework of the FP7 project CoPIRIDE, funded by the EU, novel process operations have developed in order to enable significant process intensification. High-throughput devices allow a compact, modular process design, so that the whole process can be installed inside a standard container. This concept provides a faster response to the market demands and allows shipping of the containers to places where educts are cheap and available, or the products required [1].

The often used multipurpose batch reactors allow a high number of different chemical reactions, but they are not optimized for a special chemistry and their handling provokes accidents [2]. Thus, stirred tank reactors are not feasible for fast exothermic reactions [3]. Microfluidic reactors are characterized by their enhanced heat and mass transfer rates, which is useful when researching an exothermic reaction [4]. Several working groups, e.g., Bally et al. [5] or Commenge et al. [6] have examined the advantages and the potential of microfluidic devices for highly exothermic polymerization reactions. Due to their nearly isothermal behavior and small inner dimensions, hotspots can be avoided and a fast mixing is assured. In order to control molecular weights and to gain low polydispersities, the devices have to be designed with optimum diameter and length of the channels [7].

For process intensification, the bottlenecks of conventional processes have to be identified and new types of reactions have to be investigated to make them suitable for novel process windows (NPW) [8–10]. NPW have four chemical intensification paths and two process intensification paths, as given by Hessel et al. [11]. Following the first track, a high-pressure and high-temperature approach is followed, which is best realized by combining a cold micromixer and a hot capillary reactor. Moreover, and contrary to intuition, the absence of radial mixing and thus, an ideal parabolic flow profile with full segregation of the streamlines, leads to very good performance, i.e., low polydispersity index (PDI) of the polymer produced – an effect reported by Cortese et al. for the first time [12]. The immediately high viscosity in the capillary reactor suppresses any radial diffusion and corresponding (monomer) mass transfer. Despite correspondingly

very large velocity gradients and thus residence times, each moving segment within such a microreactor has ideal reaction conditions, as there is no interference from the neighboring segment. Such a counterintuitive finding marks an NPW in the sense of process simplification.

Especially the living anionic polymerization (LAP) provides the possibility to design tailor-made polymers [13, 14] with a well-defined molecular weight and more [15] or less [16] complex molecule architecture. As monomers, commonly vinylic and aprotic molecules like styrene, isoprene, 1,3-butadiene (Bd) and others can be used. Until now, many groups have investigated the LAP and thus the effects of solvent polarity [17], initiators [18], ligands [19], and temperature [20] are well known. In the anionic polymerization of Bd as a monomer, the first addition of one monomer unit to the initiator, here *n*-butyllithium (BuLi), is the initial step, see Figure 1. It is usually much faster than the following addition of further monomers (propagation) due to the slightly higher stability of the 1,3-π-allylic complex [21, 22].

Bd can be inserted in the 1,2- or 1,4-position. The product specification of the polybutadiene often requires a certain amount of vinyl groups, because they influence the properties of the polymer, e.g., the viscosity. The fraction of $m/(m+n)$ within the whole chain quantifies the vinyl content. LAPs of Bd in pure tetrahydrofuran (THF) lead to a very high fraction of vinyl groups, because THF acts as a ligand which coordinates on the cation and thus influences the degree of delocalization of the negative charge. Thus, the ratio of ligand to initiator (L/I) strongly influences the charge distribution of the 1,3-π-allylic complex and whether the consecutive addition of the next monomer occurs on C_1 (1,4-addition) or on C_3 (1,2-addition) [23]. With cyclohexane (CHx) as the solvent and a certain amount of the ligand THF, the vinyl content can be adjusted.

Furthermore a small amount of THF is activating the initiator BuLi during the initiation step. Even a small amount of THF (L/I of at least 1) avoids oligomerization and accelerates the initiation, where BuLi is tended to oligomerization in nonpolar solvents e.g., pure CHx [24]. By using THF not only the accessibility of the monomers to the active center is increased. It avoids dimerization or higherfold oligomerization [25] of at least two living ends that are insulating the active centers [26] (Figure 2). In pure CHx, propagation is slow, but by addition of THF to

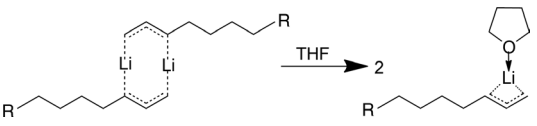

Figure 2 Avoiding of dimerization and deactivation during polymerization by using tetrahydrofuran (THF).

the reaction solution the polymerization is finished within a few min [27]. Due to the high heat removal rates microstructured or millistructured devices are suitable for handling this fast and exothermic reaction [6].

An important indicator for product quality is the PDI that is a calculated factor given by the ratio of weight and number average molar mass of a polymer sample. The PDI is a degree of conformity of the molecular weights within a polymer sample, see Eq. (1), where M_w is the mass average molar weight and M_n the number average molar weight. M_i is the molar weight of the *i*-th species, N_i is the number of molecules of species M_i in the sample. This means that in a sample, where all chains have the same molecular weight, the PDI is theoretically 1.0 [28].

$$\mathrm{PDI}=\frac{M_w}{M_n}=\frac{\Sigma M_i^2 N_i / \Sigma M_i N_i}{\Sigma M_i N_i / \Sigma N_i} \tag{1}$$

And depending on the molar fraction $\tilde{x}_i$:

$$\mathrm{PDI}=\frac{M_w}{M_n}=\frac{\Sigma M_i^2 \tilde{x}_i / \Sigma M_i \tilde{x}_i}{\Sigma M_i \tilde{x}_i / \Sigma \tilde{x}_i} \tag{2}$$

In reality, propagation underlies a statistical addition of monomers to the chain ends. Hence, product distribution for polymerization degree *P* [see Eq. (9)] follows the Poisson distribution (PD) according to Eq. (3), where $\tilde{x}_i$ is the *i*-th molar fraction.

$$\tilde{x}_i=\frac{1}{i!}P^i e^{-P} \tag{3}$$

LAP-made polybutadienes should have a PDI below 1.1 to fulfill the demand of high quality and to be suitable for specialty applications [29].

Wilms et al. [30], Wurm et al. [31], and Ziegenbalg et al. [32] showed that a very fast anionic polymerization

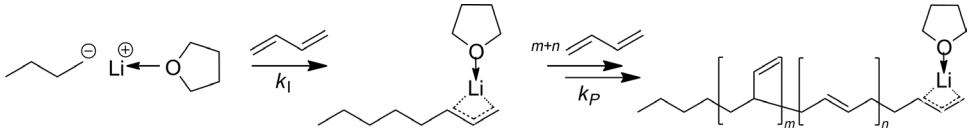

Figure 1 Reaction scheme of the anionic polymerization of 1,3-butadiene.

of styrene in pure THF can be performed in a micromixing device with molecular weights up to 70 kg mol^{-1} and polydispersities lower than 1.1. Furthermore, Nagaki et al. [33] reported on a flow rate dependency on the molecular weight distribution and that too low flow rates will lead to a broadening. Iida et al. [34] described that every kind of disruption of the flow regime in the propagation channel has to be avoided to obtain a low-PDI polystyrene or isoprene. In best cases, they obtained polystyrenes with PDI of 1.09 [33] and 1.07 [32], respectively.

In a former publication of Cortese et al. [12], computational fluid dynamics (CFD) calculations explained the dependency of PDI on microfluidics in a microchannel, with styrene as the monomer. Based on several assumptions it should be possible to obtain polystyrenes with a molar mass of up to 30,000 g mol^{-1} and a PDI of 1.03, if the mean residence time is high enough.

In this work, experimental results for an anionic polymerization of Bd in capillaries are compared with ideal reactor models and the CFD model of Cortese et al. [12].

2 Materials and methods

2.1 Setup

The setups described in literature for performing an LAP with styrene or isoprene as the monomer [29–33] are not feasible for Bd, which is gaseous at atmospheric pressure and room temperature. Figure 3 shows the flow scheme of the setup that allows a pulsation-free liquid phase polymerization. The combination of a pressurized reservoir and a mass flow controller (MFC, Bronckhorst CoriFlow mini, Wagner Mess- und Regeltechnik GmbH Offenbach/Main, Germany) has the advantage to keep and feed Bd in the liquid phase without any pulsation compared to a mechanical pump. Also, there is no possibility that cavitation occurs during the intake step.

The initiator solution and monomer solution are combined and mixed in a T-junction, with an inner diameter of 1.2 mm. In comparison to special micromixing devices like slit-interdigital or caterpillar micromixers, the T-junction proved to be less prone to clogging. The mixing device is tempered to avoid hotspots in the early state of polymerization. It is assumed that an engulfment mixing [35] is fast enough for an ideally premixed feed entering into the propagation capillary. Through a transfer pipe (d_i=0.7 mm), the reaction solution flows in the tempered propagation capillary whose dimensions (length, diameter) can be varied. An attached backpressure regulator (BPR, 7 or 17 bar) minimizes outgassing inside the propagation capillary and keeps the educts in a liquid phase. At the outlet of the capillary, the polymer is quenched with methanol and collected under methanol in a vial.

For determining the mixing quality, a setup without a propagation capillary was chosen. The BPR is directly attached to the tempered T-junction and its outlet leads immediately into a vial under methanol.

2.2 Materials

Bd (Westfalen AG, Münster, Germany, 2.5, stabilized with 1,4-tert-butylcatechol) is destabilized and dried by a

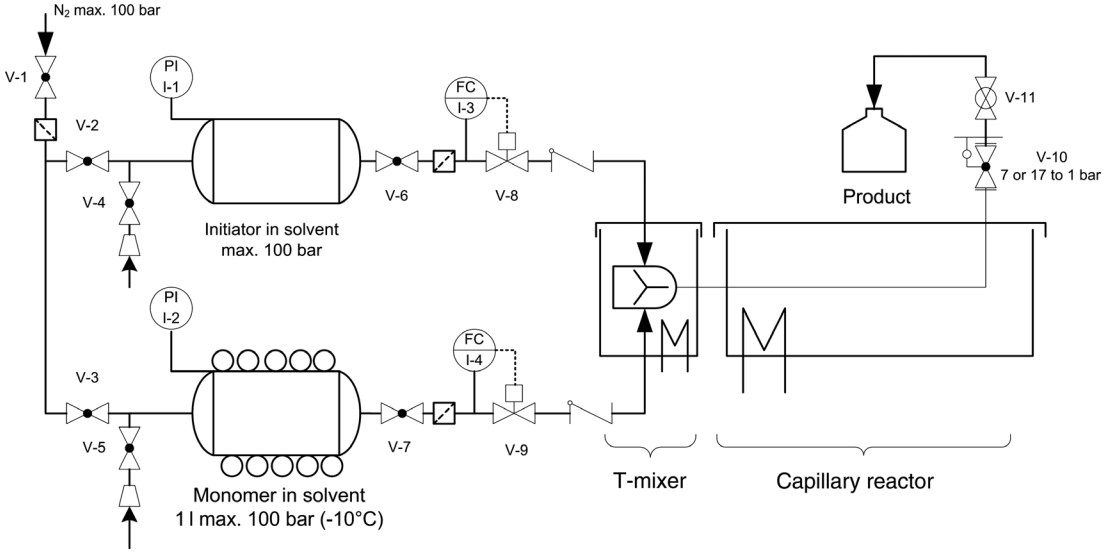

Figure 3 Flowsheet of the setup for investigations of living anionic polymerization (LAP) in continuous flow.

column of BASF (Ludwigshafen, Germany) activated alumina F-200 and a molecular sieve 4 Å. The monomer reservoir is charged with 33.9 wt% of Bd in cyclohexane (Acros Organics, Thermo Fisher Scientific, Geel, Belgium, 99.5%, extra dry, over a molecular sieve 4 Å, AcroSeal), chilled to -10°C and pressurized by 40 bar of nitrogen (Westfalen AG, 5.0). The initiator solution is prepared in a second reservoir with a 2:1 mixture of THF (Acros Organics, 99.8%, extra dry) and BuLi (Acros Organics, 1.6 M solution in n-hexane) and was consumed within 2 h, due to its high decomposition rates [36, 37]. Within 2 h, no significant decomposition of BuLi was observed, since a steady state operation also related to product specification was found. Solvents and BuLi are used without further purification. THF and CHx are checked for traces of water by Karl-Fischer-Coulometry (Metrohm 831 KF Coulometer with diaphragm, Deutsche METROHM GmbH & Co. KG, Filderstadt, Germany) and are allowed to have a maximum of 15 ppm water.

2.3 Analysis

The polymer samples are analyzed by gel permeation chromatography (GPC). As GPC-device, an Agilent 1260 (Agilent Technologies, Böblingen, Germany) Infinity Series with degasser, isocratic pump, autosampler, tempered column department, and refraction index (RI) detector is used. THF (Fisher Scientific, high pressure liquid chromatography grade) is used as an eluent, and the column is one single PLgel mixed-D, with a particle size of 5 µm. The GPC is calibrated by PSS-bdfkit [1,4-polybutadienes molar mass (M_w)=861–169,000 g mol^{-1}, by PSS Polymer Standards Service GmbH, Mainz, Germany]. With the help of the WinGPC-PlugIn for Agilent ChemStation, M_w and PDIs are determined.

By head-space gas chromatography (GC), the mixing quality was determined with an HP 5860 Series II, equipped with a 50 m PONA column, hydrogen as a carrier gas, and a split of 1:400. The initial temperature is 35°C held for 3 min, with an additional heating up to 60°C during the following 8 min. The signal areas are calculated by the ChemStation software. The ratios of the integrals of Bd to CHx signals and butane to n-hexane signals are manually calculated.

2.4 Experimental procedure

2.4.1 Investigation of mixing quality

For investigation of the mixing quality, the setup without a propagation capillary is used. The temperature of the mixing device is set to T_{mix}=-10°C, 0°C, and 25°C, with the mass flow rates $\dot{m}_I$ =15 g h^{-1} for the initiator solution and $\dot{m}_M$ =15 g h^{-1}, 30 g h^{-1}, and 60 g h^{-1} for the monomer solution. Both of the inlet channels were measured in single mode in order to determine the concentrations in the reservoirs. After steady-state was reached, a head-space gas sample (5 µl) was taken from the sample glass with a gas syringe and injected into the GC.

2.4.2 Variation of capillary length

For polymerization, the temperature of the mixing device is T_{mix}=25°C and the capillary temperature is T_{cap}=45°C. Mass flow rates of $\dot{m}_I$ =15 g h^{-1} for the initiator solution and $\dot{m}_M$ =60 g h^{-1} for the monomer solution are chosen (Table 1). Four capillaries with an inner diameter of d_i=1.75 mm and an inner volume of V_{cap}=2 ml, 4 ml, 6 ml, and 8 ml are used while the outlet pressure is p_{BPR}=7 bar. The procedure starts with running the setup for at least 15 min until steady-state is reached. Subsequently, samples are taken every 5 min. The vials are filled with additional methanol and the polymer is settled overnight. Then, the solvent is decanted and the residual polymer is dried by evacuation in an exsiccator for at least 6 h at p_{vac}<2 mbar.

2.4.3 Variation of reaction temperature

Generally the same procedure was performed as for the variation of capillary length, but only the 4 ml capillary was used and the temperature T_{cap} is varied in steps of 15°C, from 30°C to 90°C. To keep the Bd in the liquid phase, the outlet pressure was increased to p_{BPR}=17 bar. The work-up of the polymer followed the steps described above.

2.5 Modeling

2.5.1 Kinetic modeling

LAP is a strictly linear addition of the monomers. Chain transfer reactions and untimely terminations of the

Table 1 Settings for the continuous flow setup.

	Monomer solution	Initiator solution
Content	33.9 wt% Bd in CHx	10 ml n-BuLi 1.6 M in 20 ml THF
Mass flow rates	60 g h^{-1}	15 g h^{-1}
Density ρ	725 kg m^{-3}	810 kg m^{-3}

Bd, 1,3-butadiene; BuLi, n-butyllithium; CHx, cyclohexane; THF, tetrahydrofuran.

propagation do not occur. Eq. (4) describes the propagation, where P_i is the i-th polymer species and M the monomer. The reaction rate r obeys a first order kinetics, both related to the monomer and the polymer chain and is calculated according to Eq. (5), where c_M is the concentration of the monomer, c_{P_i} the concentration of the growing polymer chain with chain lengths of i monomers and k_P the propagation rate constant.

$$\begin{aligned} P_0 + M &\longrightarrow P_1 \qquad r_0 = k_P c_{I,0} c_{M,0} \\ P_1 + M &\longrightarrow P_2 \qquad r_1 = k_P c_{P1} c_M \\ &\cdots \\ P_{i\text{-}1} + M &\longrightarrow P_i \qquad r_{i\text{-}1} = k_P c_{P_i\text{-}1} c_M \end{aligned} \tag{4}$$

$$r_i = k_P c_{P_i} c_M \tag{5}$$

Thus, the concentration of active sites $c_{\Sigma P\text{-}}$ is constant and equates to the starting concentration of the initiator $c_{I,0}$ under inert conditions [Eq. (6)]. Furthermore, the initiation step (k_I) is much faster than the following propagation (k_P) [Eq. (7)], and it is assumed that initiation only takes place in the mixing device. Thus, the initiation step is negligible in the polymerization kinetics. In most cases, the consumption of the monomer can be described with a pseudo-first order kinetics following Eq. (8), where $c_{M,t}$ is the time-related concentration of residual monomer, $c_{M,0}$ the starting concentration, and τ the residence time.

$$c_{I,0} = c_{\Sigma P\text{-}} \tag{6}$$

$$k_I >> k_P \tag{7}$$

$$c_{M,t} = c_{M,0} e^{-k_P c_{I,0} \tau} \tag{8}$$

Due to the difficulty of determining the residual Bd, $c_{M,t}$ can be calculated from the polymer formed. $c_{M,0}$ is known, the average molar mass M_w of the polymer sample is a result of the GPC analysis, so the percentage of the consumed monomer is calculated with the help of the mean P, that gives the number of the monomer units in a polymer chain:

$$P = \frac{M_w - M_{\text{butyl}}}{M_{\text{Bd}}} \tag{9}$$

The ratio of the P of the sample, P_{sample}, and the theoretical polymerization degree $P_{\max}$ corresponding to full conversion of the monomer, gives the conversion of the monomer X_M [Eq. (10)].

$$X_M = \frac{P_{\text{sample}}}{P_{\max}} \tag{10}$$

The propagation rate constant k_P can be calculated according to Eq. (11):

$$k_P = \frac{1}{c_{I,0}\tau} \ln\left(\frac{c_{M,t}}{c_{M,0}}\right) = \frac{1}{c_{I,0}\tau} \ln(1 - X_M) \tag{11}$$

with Eq. (12).

$$\frac{c_{M,t}}{c_{M,0}} = X_M \tag{12}$$

2.5.2 Reactor modeling

In the first two simulations, an ideal plug flow reactor (PFR) and an ideal laminar flow reactor (LFR) are assumed. It sets the focus on a simple PDI modeling for anionic polymerization in tubular reactors. The most simplified model is to assume the tubular reactor as a single PFR. There is no interaction between wall and fluid, thus, there is no difference in individual residence times. The molar mass distribution of a polymerization in a PFR must be equal to the PD.

In the second simulation, the LFR with a parabolic flow profile is assumed, which causes a broad residence time distribution. With the simplification that a mean flow velocity can be attributed to every shell, each shell is modeled by a PFR.

These two simulations are calculated with some simplifying general assumptions: during the polymerization density, diffusivity, and viscosity will not change and the reaction rate constant k_P is independent from the degree of conversion or chain length. Furthermore, initiation is completed and the propagation starts homogeneously at the inlet of the capillary (z=0). Finally, the polymerization solution behaves as a Newtonian fluid. Influence of discretization is step size tested.

The third simulation based on CFD examines the fluid dynamic (FD) impact on the PDI. It sets its focus on the properties of the reaction solution that are changing with the chain length of the polybutadienes. At the outlet, the PDI is calculated from the sum of all obtained molecular weights M_w.

2.5.2.1 Ideal PFR model

A single ideal PFR provides a simplified model of the polymerization in a capillary and supplies information on statistical PDI development, excluding FD effects, but including a full cross-mixing. Therefore, a first

order kinetic is assumed following the reaction scheme described by Eq. (4). The reaction rate r_p is calculated by Eq. (5), with k_p being the rate constant.

$$\frac{dc_{P_i}}{dz}=\frac{1}{v}(r_{i-1}-r_i) \tag{13}$$

Eq. (13) is the mass balance of the ideal PFR which describes the formation and consumption of the polymer with chain length i along the capillary. The mass balance is solved with the help of MATLAB ODE-solver (MathWorks, Ismaning, Germany). The concentrations of the species P_i give the molecular weight distribution at the corresponding position along the axis and the mean P. The PDI is calculated by Eq. (1).

This simulation is compared to the PD that is given by Eq. (3) for the molar fraction $\tilde{x}$ depending on the P.

2.5.2.2 Ideal LFR model

For the ideal LFR, the parabolic flow profile is divided into shells. Each shell is modeled as a single PFR, assuming that there is no mass transport by diffusion between the streamlines (full segregation), see Figure 4. At the outlet of the capillary, all polymers obtained in each shell are summed up and give the average PDI.

The flow velocities $v(r_{cap})$ of the parabolic profile are calculated by Eq. (14), where v_{avg} is the average flow velocity, r_{cap} the radial position in the capillary, and R_{cap} the entire radius of the capillary.

$$v(r_{cap})=2\,v_{avg}\left(1-\left(\frac{r_{cap}}{R_{cap}}\right)^2\right) \tag{14}$$

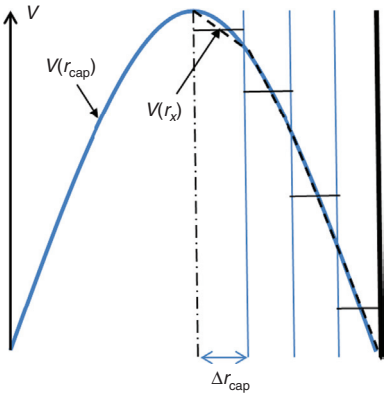

Figure 4 Scheme of the flow profile in an ideal laminar flow reactor (LFR).

The tube is divided into N shells having a width Δr_{cap} according to Eq. (15).

$$\Delta r_{cap}=R_{cap}/N \tag{15}$$

The local mean flow velocity in the shell, $v(r_x)$, is calculated as follows:

$$v(r_x)=0.5\cdot(v(r_{x+1/2})+v(r_{x1/2})) \tag{16}$$

Each shell is modeled as an ideal PFR. At axial reactor position z, the mass balance according to Eq. (13) is solved for each shell. The flow rates of each polymer species P_i, the local mean molar masses, and the PDI are calculated with Eqs. (17)–(20). This finally leads to the mean PDI of all shells by summing over the cross section to get the total flow rate of each species [Eq. (20)].

$$\dot{n}_{P_i}(z)=\Sigma_x\dot{n}_{P_i}(x,z) \tag{17}$$

$$M_n(Z)=\frac{\Sigma_i M_{P_i}^2\dot{n}_{P_i}(z)}{\Sigma_x\dot{n}_{P_i}(z)} \tag{18}$$

$$M_w(Z)=\frac{\Sigma_i M_{P_i}^2\dot{n}_{P_i}(z)}{\Sigma_x M_{P_i}\dot{n}_{P_i}(z)} \tag{19}$$

$$\mathrm{PDI}(z)=\frac{M_w(z)}{M_n(z)} \tag{20}$$

2.5.2.3 CFD model

In contrast to the simplified PFR models, the CFD model includes changes in fluid properties, like viscosity, diffusivity, thermal conductivity, and heat capacity correlating to the molecular weight M_w of the polymer chain. The dependences of the viscosity and the diffusivity of the reaction solution on the molecular weights of polybutadienes in CHx as the solvent are shown in Figure 5. The intrinsic viscosity is calculated by the Han equation [38] as a function of molecular weight of the polymer with the dataset of Mello et al. [39]. The diffusion coefficient is correlated to the solution viscosity by means of the Hayduck-Cheng equation [40] using as a starting data-set the values reported by Chalykh et al. [41].

The methodology for the calculations is described in more detail by Cortese et al. [12]. Like the other simulations, the CFD calculations presume an ideally premixed feed at the inlet and an isothermal reaction. To avoid a virtual clogging in the capillary, a slip flow at the wall is introduced. It is assumed that the polymer is not diffusing. The calculations are performed with COMSOL (Comsol Inc., Los Angeles, CA, USA), 4.3.0.151. Due to the high computing effort, the capillary was scaled to a shorter one, but

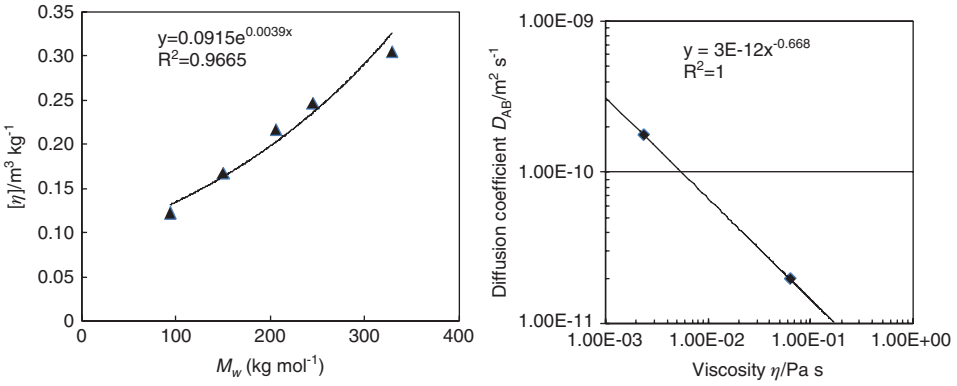

Figure 5 Effect of molecular weight M_w on viscosity and diffusion of the reaction solution.

checked for comparability to the capillary with a length of 3.28 m.

3 Results and discussion

3.1 Premixing and initiation

In all the reactor models used in this work, an ideally premixed feed with completed initiation entering the propagation capillary is assumed. Therefore, the setup without the propagation capillary is used to gain insight into the state of the polymerization before entering the propagation capillary. The amount of unconverted BuLi cannot be analyzed directly, but the protonated product n-butane is separable from to Bd on a nonpolar PONA column by GC. However, it is difficult to get a concrete quantitative conclusion from an analysis of a pressurized gas/liquid product system, due to the complex gas/liquid equilibria after expansion. Furthermore, the untimely decomposed BuLi also forms butane, which is carried through the setup ($A_{\mathrm{Bu},x}$). For a semi-quantitative investigation, the relative head-space GC method, where the ratios of signal-areas of butane to hexane and butadiene to CHx, respectively, are examined, is sufficient. The conversion of BuLi X_{BuLi} is given by Eq. (21), with $\frac{A_{\mathrm{Bu,tot}}}{A_{\mathrm{nHx,tot}}}$ as the total relative amount of butane formed by the initiator solution after methanolysis, $\frac{A_{\mathrm{Bu},x}}{A_{\mathrm{nHx},x}}$ as the value of pre-decomposed BuLi taken from the gas phase in the feed reservoir, and $\frac{A_{\mathrm{Bu},t}}{A_{\mathrm{nHx},t}}$ as the measured value of the residual amount of BuLi which was not converted with Bd in the mixer.

$$X_{\mathrm{BuLi}} = \frac{\frac{A_{\mathrm{Bu,tot}}}{A_{\mathrm{nHx,tot}}} - \frac{A_{\mathrm{Bu},x}}{A_{\mathrm{nHx},x}} - \frac{A_{\mathrm{Bu},t}}{A_{\mathrm{nHx},t}}}{\frac{A_{\mathrm{Bu,tot}}}{A_{\mathrm{nHx,tot}}} - \frac{A_{\mathrm{Bu},x}}{A_{\mathrm{nHx},x}}} \tag{21}$$

For Bd, the conversion is calculated by Eq. (22), with the signal areas $A_{\mathrm{Bd,tot}}$ of Bd in the headspace of the feed reservoir and $A_{\mathrm{Bd},t}$ after reaction with BuLi in the mixer.

$$X_{\mathrm{Bd}} = \frac{\frac{A_{\mathrm{Bd,tot}}}{A_{\mathrm{CHx,tot}}} - \frac{A_{\mathrm{Bd},x}}{A_{\mathrm{CHx},t}}}{\frac{A_{\mathrm{Bd,tot}}}{A_{\mathrm{CHx,tot}}}} \tag{22}$$

The conversion for three different residence times is measured at three temperatures (T_{mix}=-10°C, 0°C, and 25°C). Figure 6 shows no further increase of conversion exceeding 0°C. Even a residence time of τ=18 s is not leading to significantly higher conversion of BuLi. Thus, it can be

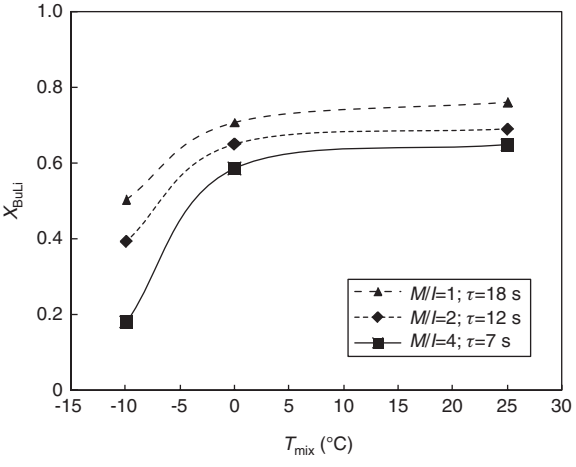

Figure 6 Conversions of n-butyllithium in the mixing device at different temperatures, residence times and monomer/initiator ratios.

assured that initiation is completed when entering the capillary. The deviations of the expected full conversions at high temperatures and residence times are caused by the semi-quantitative approach due to the headspace measurements.

For the conversion of X_{Bd}, it is shown in Figure 7 that up to a residence time of τ=12 s at T_{mix}=25°C, only a small amount of X_{Bd}<10% is converted, or has been added to the initiator. With a higher residence time (τ=18 s), a higher amount of Bd is converted.

It can be concluded that a mixing temperature of 25°C and mass flow rates of $\dot{m}_I$ of 15 g h^{-1} for the initiator solution and $\dot{m}_M$ of 60 g h^{-1} for the monomer solution leads to a sufficient separation of initiation and propagation steps. Therefore, the boundary condition for the reactor models is fulfilled.

3.2 Intrinsic kinetics

For the anionic polymerization of Bd initiated by BuLi in a solvent mixture of CHx and THF, the activation energy E_A and the pre-exponential factor $k_{P,inf}$ can be determined by variation of the temperature. The experiments are carried out in the described setup, with a capillary of V_{cap}=4 ml (l_{cap}=1.66 m, d_i=1.75 mm) and a BPR with p_{BPR}=17 bar. With a total mass flow rate of $\dot{m}_{tot}$=75 g h^{-1}, the calculated arithmetic mean density of ρ_{tot}=742 kg m^{-3} gives a residence time of τ=152 s, including the transfer pipes and the inner volume of the BPR. The elevated pressure is necessary to keep Bd in a liquid phase above 45°C. Compared to experiments performed at T_{cap}=30°C or 45°C and p_{BPR}=7 bar, the polymers show nearly the same molecular weights M_w (Table 2). Higher outlet pressures guarantee a liquid phase in the capillary, even at higher reaction temperatures, but setting the steady state demands higher efforts in handling.

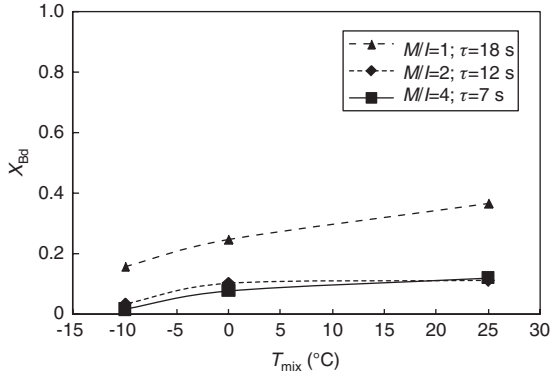

Figure 7 Conversion of 1,3-butadiene in the mixing device at different temperatures, residence times and monomer/initiator ratios.

Table 2 Comparison of selected polybutadienes obtained at different pressures p_{BPR}.

	p_{BPR}=7 bar M_w (g mol^{-1})	p_{BPR}=17 bar M_w (g mol^{-1})
T_{cap}=30°C	6336	6182
T_{cap}=45°C	8860	8742

M_w, weight average molar mass; p_{BPR}, pressure at the outlet of the capillary; T_{cap}, wall temperature of the capillary.

Figure 8 shows the obtained molar masses M_w of the samples for each reaction temperature. For the calculation of every particular propagation rate k_P, an ideal PFR is assumed and Eq. (11) is applied. The average molar mass of each run is taken.

According to the Arrhenius equation [Eq. (23)], the activation energy is E_A=22.0 kJ mol^{-1} and the pre-exponential factor is $k_{P,inf}$=94,100 l mol min^{-1}.

$$k_P = k_{p,inf} e^{-E_A/RT} \tag{23}$$

In the following, k_P=25 l mol^{-1} min^{-1} corresponding to 45°C is used for the simulations.

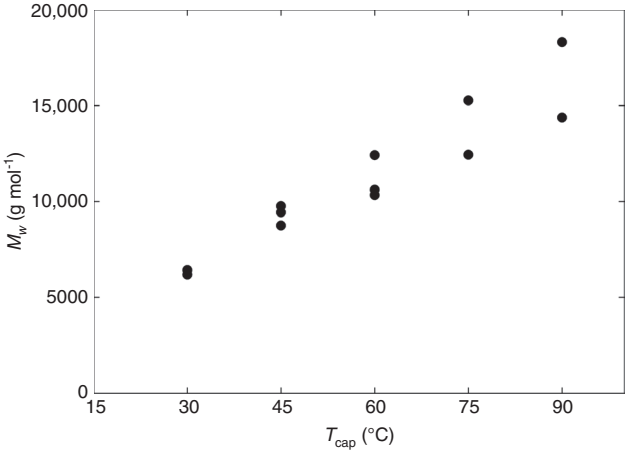

Figure 8 Molar masses of polybutadienes obtained at different T_{cap} (experimental details see Tables 1 and 3).

Table 3 Experimental results and determined k_P.

T_{cap} (°C)	$M_{w,av}$ (g mol^{-1})	P (-)	X_{Bd} (-)	k_P (l mol min^{-1})
30	6299	116	0.31	15±0.5
45	9309	171	0.46	25±1.5
60	11,119	205	0.55	32±4
75	13,850	255	0.68	46±7
90	16,343	302	0.80	66±10

k_P, propagation rate constant; $M_{w,av}$, weight average molar mass; P, polymerization degree; T_{cap}, wall temperature of the capillary; X_{Bd}, conversion of Bd.

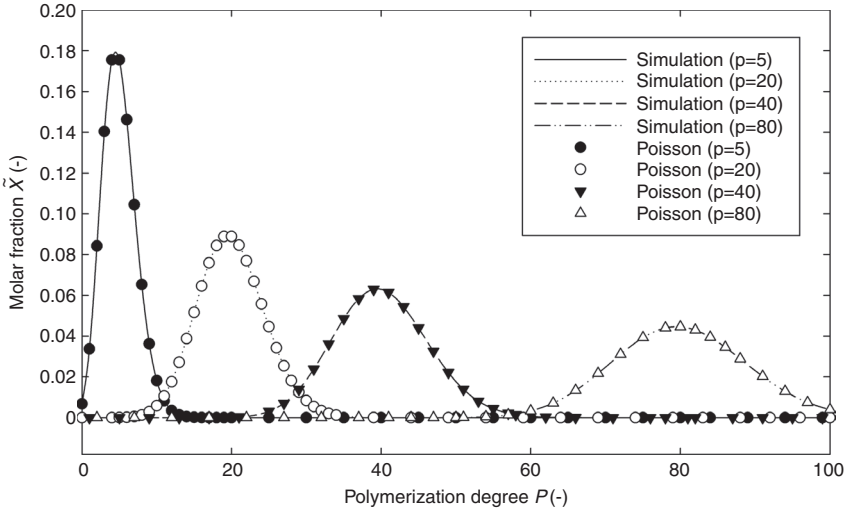

Figure 9 Molecular weight distribution of an ideal plug flow reactor (PFR) versus Poisson distribution of selected polymers with polymerization degrees P in brackets.

3.3 Determining the PDI

3.3.1 Ideal PFR model

Figure 9 shows the distributions of molar fractions of polymers with the mean polymerization degrees P=5, 20, 40, and 80, the so-called PD following Eq. (3) and the simulation based on Eqs. (5) and (13), with the rate constant determined beforehand. The resulting curves are matching exactly. Thus, under ideal and simplified conditions, the PDI in a PFR is calculable only by the molar fraction combining Eqs. (2) and (3).

Usually PDIs at lower polymerization degrees are higher, due to the fact that one more or less monomer unit effects are more noticeable at lower than at higher polymerization degrees. With Eq. (13) and with the determined rate constant, the resulting molar weights of the i-th polybutadiene species are calculated. The PDIs are determined according to Eq. (2) and are plotted versus the normalized reactor length, see Figure 10. The normalization is necessary for model comparison, because the simulation uses the capillary geometry and reaction parameters of the experiments. It is shown that the lowest obtainable PDI is about 1.015 for a polymerization degree of about 250 at the outlet and falls below 1.02 after about 15% of the reactor length.

3.3.2 Ideal LFR model

This model gives a slower decrease of the PDI along the propagation capillary compared to the single PFR, where the reactor length is normalized on the length of the capillary (3.28 m) (Figure 11). The PDI course falls below 1.02 after 60% of the entire capillary length and the PDI decreases consecutively to 1.015 at the outlet.

3.3.3 CFD model

The results of the 3D CFD simulations using the overall kinetics $r=k_P\, c_{I,0}\, c_M$ are shown in Figure 12. Due to the very time-consuming calculations, only two 3D results were created. For the CFD results, PDIs are higher than in the ideal PFR or LFR models. It shows that PDI is dependent on FD as well as statistical effects (PD). The statistics

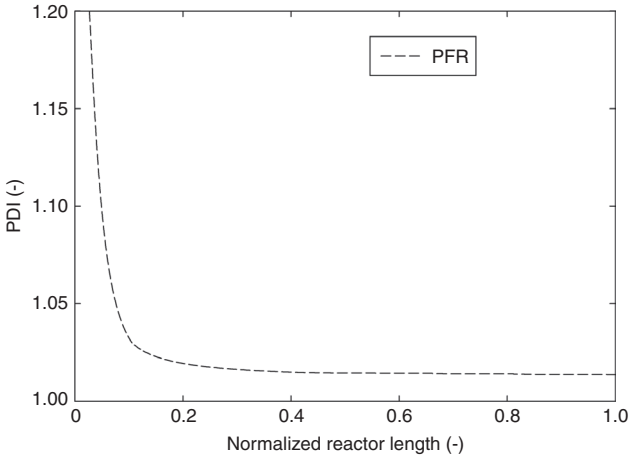

Figure 10 Polydispersity index (PDI) versus reactor length for an ideal plug flow reactor (PFR) model.

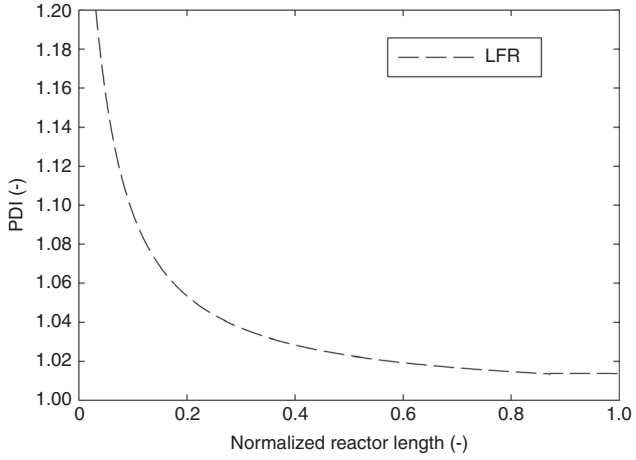

Figure 11 Polydispersity index (PDI) versus reactor length for an ideal laminar flow reactor (LFR) model.

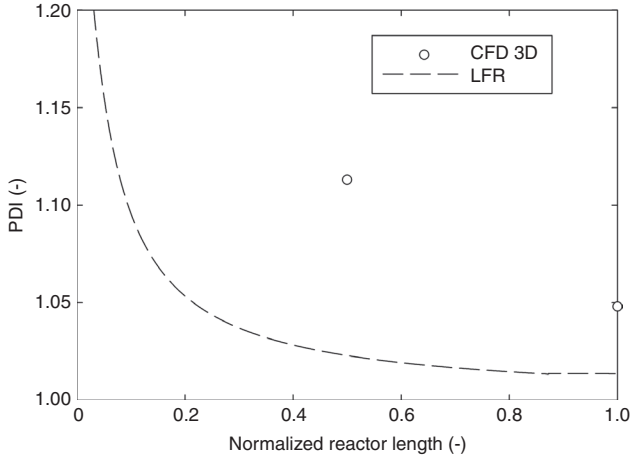

Figure 12 Polydispersity index (PDI) versus reactor length for computational fluid dynamics (CFD) model and laminar flow reactor (LFR) model.

influence the most to the final PDI, while FD alone contributes, adding 0.015 to the total PDI in a continuous set-up (Table 4).

Table 4 Parameters and results for computational fluid dynamics (CFD) 3D simulations.

τ (s)	k_p (l mol^{-1} min^{-1})	X_{Bd} (%)	M_w (g mol^{-1})	PDI_{CFD}	PDI_{CFD+PD}
75	25	19	5350	1.013	1.113
150	25	34	9460	1.012	1.041

CFD, computational fluid dynamics; k_p, propagation rate constant; M_w, weight average molar mass; PD, Poisson distribution; PDI, polydispersity index; τ, residence time; X_{Bd}, conversion of Bd.

In the calculations it is shown that a segregated flow regime is prevailing. The diffusion coefficient D_{AB} is in the order of 10^{-11} m^2 s^{-1} in the blue area in Figure 13; the Fourier number (Fo) suggests with values of about Fo=0.01, that the streamlines are segregated. According to Einstein's equation, see Eq. (24), the mean diffusion length for Bd $<\Delta l>$ is about 10 µm at the outlet of the capillary. Compared to the inner diameter of the propagation capillary with 1.75 mm the diffusion is negligible low. Thus the streamlines are practically independent.

$$<\Delta l>=\sqrt{2D_{AB}\tau} \tag{24}$$

However, the high diffusion fluxes at the walls, described by the red area in Figure 14, should give the reason for increased PDIs of the CFD results. Although the streamlines can be assumed as almost segregated in consideration of diffusion constants, the monomer concentration gradients increase towards the wall. This effect is not described by the ideal segregated flow in the LFR model. Elevated monomer diffusion fluxes from the center to the wall affect a change on the ratio of the monomer to the living polymer chain ends or rather initiator [M/I, with Eq. (6)] in the ideally premixed volume units. The consecutive fading into blue describes the slow-down of the diffusion and diffusion fluxes and therefore the ratios of the monomer to the polymer anion are frozen on the streamlines. This leads to deviations in the polymerization degrees and a higher PDI.

3.4 Comparison with experimental results

For investigation of the development of PDI during the polymerization, the results of the experimental variation of the capillary length are shown in Figure 15. Only the two lowest PDIs of obtained polybutadienes of each capillary length are chosen. They mark the lower limit. Other values are neglected, due to the high sensitivity of PDI on every deviation from the steady state.

Obviously, there is an experimental limit with at a PDI of about 1.04 for molecular weights up to 16,500 g mol^{-1}. Compared to the results in the ideal PFR or the ideal LFR, the experimental PDIs are still too high. As expected, the PFR describes the PD. The LFR model gives PDIs which are slightly closer to the experimental data, but nevertheless still significantly lower by an absolute value of about 0.02. Compared to the PFR model, the LFR model gives higher PDI values due to the segregated flow. For very high residence times, the courses of the ideal PFR and LFR models approach to the same boundary value, the PD, which also

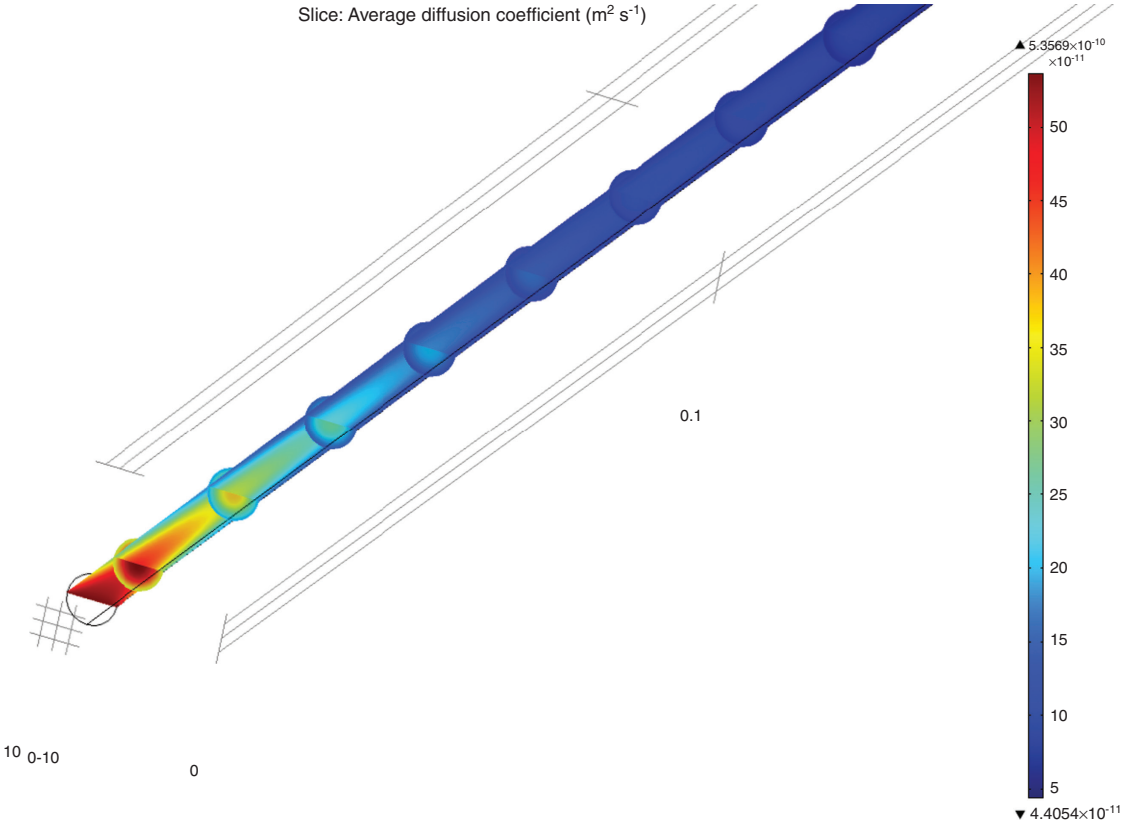

Figure 13 Computational fluid dynamics (CFD) simulation of diffusion constants of 1,3-butadiene in $m^2 s^{-1}$.

confirms the work of Cortese et al. [12], where segregated flow and a high residence time lead to very low PDI. The PFR and the LFR approaches give the right tendency, but do not reflect the real behavior. Considering only the statistical effects, the lower limit of PDI is about 1.02. The experimental results must contain an additional influencing value due to a not fully segregated flow. Moreover, CFD simulations suggest that a further value of 0.015 has to be added to the statistical PDI, due to the described effects of higher monomer concentration gradients towards the wall

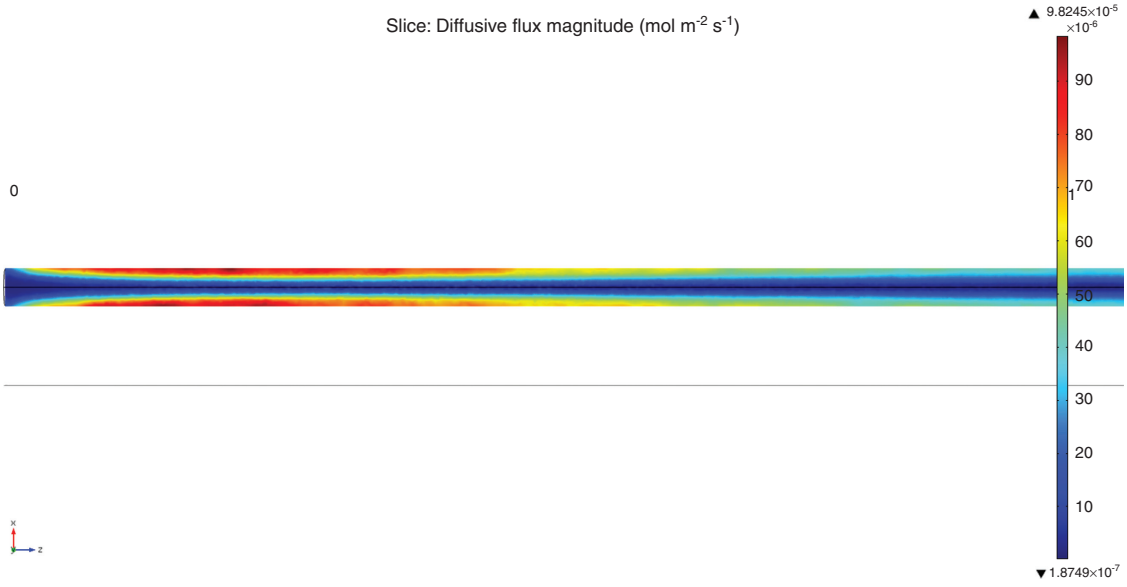

Figure 14 3D computational fluid dynamics (CFD) simulation of the diffusive flux of 1,3-butadiene in mol $m^{-2} s^{-1}$.

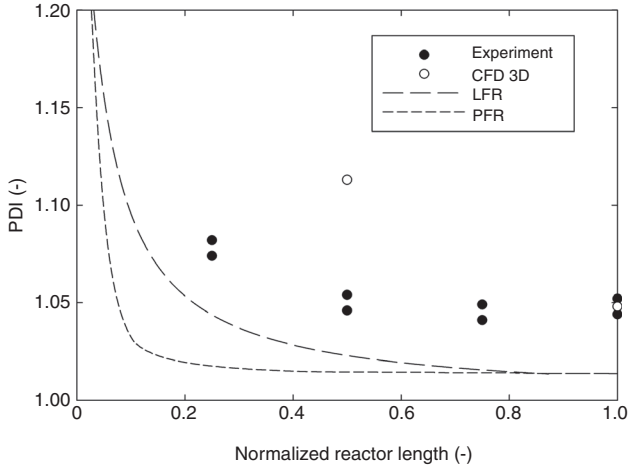

Figure 15 Polydispersity index (PDI) values of polybutadienes obtained from different capillary lengths.

and the consecutive freezing of the disarranged monomer to initiator ratios. As boundary conditions neither full cross-diffusion (PFR) nor fully segregated flow (LFR) are fulfilled. Thus, the sum of FD effects and the statistics lead to realistic PDI values that can be observed in experimental results in a continuous microfluidic setup.

The comparison of the obtained polymers and PDIs with the results of other groups shows that there are advantages of the used setup. Avoiding pulsation and the combination of a chilled mixing device and a heated capillary outperforms the hitherto existing setups (Table 5). A separation of mixing and further propagation in a segregated flow causes a decrease of the PDI.

4 Conclusions

With the help of experiments and simulations, it can be shown that the resulting PDI of a polymer made by LAP consists of FD and a statistical part. The FD contribution increases the PDI only by a value of about 0.015. More dominating is the statistical effect that obeys the PD and limits the PDI to 1.02 for anionic polymerizations up to a molar weight of 16,500 g mol^{-1} in a microfluidic system with the investigated chemistry and setup. With the help of CFD modeling, it is shown that neither an infinite dispersion across the cross section (ideal PFR model) nor a fully segregated flow regime (ideal LFR model) exists. High diffusion fluxes near the wall at the inlet of the propagation capillary effect changes in the ratio of monomer to initiator. This leads to inhomogeneous polymerization degrees and therefore a broader distribution of the molecular weights of the polymer. Nevertheless, in summary, a PDI of 1.035 marks a realistic value that can definitely be achieved. Thus, a continuous microfluidic flow reactor can provide a low-PDI polymer that is comparable to polymers that are made in a batch reactor.

The combination of a pulsation free dosing and the use of a chilled mixing device and a heated capillary can provide low-PDI polybutadienes and outperforms the existing setups. This gives the opportunity for process intensification by a transfer from a semi-batch operation into a continuous microfluidic reactor, while maintaining the product quality.

Symbols

Symbol, Unit	Description
A	Integrated signal area at GC measurements
C, mol l^{-1}	Concentration
$D_{AB,}$ m^2 s^{-1}	Diffusion coefficient
d, m	Diameter
Fo	Fourier number ($Fo=D_{AB}\tau\, l^{-2}$)
i	Counter variable, regarded species
$k_{i,}$ l mol^{-1} min^{-1}	Initiation rate constant

Table 5 Summary and comparison of literature results for living anionic polymerization (LAP) in microreactors.

Ref.	Setup/mixer	Monomer	Solvent	$V_{M/I}$ (ml min^{-1})	T_R (°C)	M_w (g mol^{-1})	Lowest PDI
[30, 31]	SIMM	Styrene	THF	–	25	11300	1.09
[30, 31]	SIMM+Cap.	Styrene	CHx	–	25	8000	1.08
[32]	Caterpillar	Styrene	CHx	1.99/0.026	25	6000	1.07
[33]	T-junc.+Cap.	Styrene	THF	6.0/2.0	-28	3600	1.07
[33]	T-junc.+Cap.	Styrene	THF	6.0/2.0	0	3200	1.08
[34]	T-junc.+Cap.	Styrene	CHx	0.017/0.017	35	5300	1.09
[34]	T-junc.+Cap.	Isoprene	CHx	0.008/0.008	30	8300	1.10
This Work	T-junc.+Cap.	Butadiene	CHx/THF	1.33/0.33	45	9500	1.04

CHx, cyclohexane; M_w, weight average molar mass; PDI, polydispersity index; T_R, reaction temperature; THF, tetrahydrofuran; SIMM: Slit Interdigital Micromixer (IMM Mainz GmbH, Mainz, Germany); Cap., Capillary; T-junc., T-junction.

k_P, l mol^{-1} min^{-1}	Propagation rate constant
$k_{P,inf}$, l mol^{-1} min^{-1}	Pre-exponential factor
l, M	Characteristic length
L/I	Ligand to initiator ratio (THF/BuLi)
m, G	Mass
$\dot{m}$, g h^{-1}	Mass flow rate
M, g mol^{-1}	Molar mass
M_n, g mol^{-1}	Number average molar mass
M_w, g mol^{-1}	Weight average molar mass
M/I	Monomer to initiator ratio (Bd/BuLi=Bd/P$^-$)
n, Mol	Molar amount of matter
$\dot{n}$, mol s^{-1}	Molar flow rate
N	Discretization step in axial direction
N_i	Number amount of species i
p_{BPR}, Bar	Pressure at the outlet of the capillary
P	Polymerization degree
PDI	Poly dispersion index (M_n/M_w)
r, m	Radius (variable)
r, mol l^{-1} min^{-1}	Reaction rate
R, J mol^{-1} K^{-1}	Gas constant (8.3141 J mol^{-1} K^{-1})
T_{cap}, °C	Wall temperature of the capillary
T_{mix}, °C	Temperature of the mixing device
T_R, °C	Reaction temperature
t, S	Time
v, m s^{-1}	Velocity
$\dot{V}$, cm^3 s^{-1}	Volume flow rate
V_R, cm^3	Reaction volume
x	Coordinate in radial direction
X	Conversion degree
$\tilde{x}$	Molar fraction

Greek symbols

Symbol, Unit	Description
η, Pa s	dynamic viscosity
$[\eta]$, Pa s	intrinsic viscosity
ρ, kg m^3	density
τ, s	residence time

Abbreviations

Abbreviation	Description
Bd	1,3-butadiene
BPR	backpressure regulator
BuLi	*n*-butyllithium
cap	(concerning) capillary
CFD	computational fluid dynamics
CHx	cyclohexane
FD	fluid dynamics
GC	gas chromatography
GPC	gel permeation chromatography
HPLC	high pressure liquid chromatography
I	initiator
L	ligand
LAP	living anionic polymerization
LFR	laminar flow reactor
M	monomer
nHx	n-hexane
P	polymer
P$^-$	polymer anion
PD	Poisson distribution
PDI	polydispersity index
PFR	plug flow reactor
TBC	1,4-tert-butylcatechol
THF	tetrahydrofuran

Acknowledgement: The research leading to these results has received funding from the European Community's Seventh Framework Programme [FP7/2007–2013] under grant agreement no. CP-IP 228853-2.

Received July 15, 2013; accepted August 21, 2013; previously published online September 18, 2013

References

[1] www.copiride.eu (July 2013).
[2] Schnyder A. „Chemische Prozesse in Mehrproduktanlagen sicher fahren", Jubiläumspublikation 15 Jahre Schnyder Sicherheit in der Chemie AG, 2002, 1–50.
[3] Hugo P, Lopez F. *Chem. Ing. Tech*. 2009, 81, 145–152.
[4] Jähnisch K, Hessel V, Löwe H, Baerns M. *Angew. Chem. Int. Ed*. 2004, 43, 406–446.
[5] Bally F, Serra CA, Hessel V, Hadziioannou G. *Chem. Eng. Sci.* 2011, 66, 1449–1462.
[6] Commenge JM, Falk L, Corriou JP, Matlosz M. *Chem. Eng. Technol*. 2005, 28, 446–458.
[7] Tonhauser C, Natalello A, Löwe H, Frey H. *Macromolecules* 2012, 45, 9551–9570.
[8] Hessel V, Cortese B, de Croon MHJM. *Chem. Eng. Sci.* 2011, 66, 1426–1448.
[9] Hessel V, *Chem. Eng. Technol.* 2009, 32, 1655–1681.
[10] Lomel S, Falk L, Commenge JM, Houzelot L. *Chem. Eng. Res. Des.* 2006, 84, 363–369.

[11] Hessel V, Kralisch D, Kockmann N, Noël T, Wang Q. *ChemSusChem* 2013, 6, 746–791.
[12] Cortese B, Noël T, de Croon MHJM, Schulze S, Klemm E, Hessel V. *Macromol. React. Eng.* 2012, 6, 507–515.
[13] Szwarc M. *Nature* 1956, 178, 1168–1169.
[14] Quirk, RP. In *Encyclopedia of Polymer Science and Technology*, John Wiley & Sons, Inc.: New York, 2002.
[15] Hajichristidis N, Pitsikalis M, Pispas S, Iatrou H. *Chem. Rev.* 2001, 101, 3747–3792.
[16] Halasa AF, Lohr DF, Hall JE. *J. Polym. Sci., PCE Ed.* 1981, 19, 1357–1360
[17] Essel A, Salle R, Golé J, Pham QT. *J. Polym. Sci. PCE* 1975, 13, 1847–1853.
[18] Hsieh HL. *J. Polym Sci, Pt. A* 1966, 3, 163–172.
[19] Antkowiak TA, Oberster AE, Halasa AF, Tate DP. *J. Polym. Sci. Pt. A* Vol. 1972, 10, 1319–1334.
[20] Uraneck CA. *J. Polym. Sci. Pt. A* 1971, 9, 2273–2281.
[21] Morton M, Sanderson RD, Sakata R. *Polym. Lett.* 1971, 9, 61–70.
[22] Morton M, Fetters LJ. *Rubber Chem. Technol.* 1975, 48, 359–409.
[23] Halasa AF, Schulz DN, Tate DP, Mochel VD. *Adv. Organomet. Chem.* 1980, 18, 55–97.
[24] Bywater S, Worsfold DJ. *J. Organomet. Chem.* 1967, 10, 1–5.
[25] Worsfold DJ, Bywater S, *Macromol.* 1972, 4, 393–397.
[26] Bywater S, Worsfold DJ, Hollingsworth G. *Macromol.* 1972, 4, 389–393.
[27] Chang CC, Miller Jr. JW, Schorr GR. *J. Appl. Polym. Sci.* 1990, 39, 2395–2417.
[28] Young RJ, Lovell PA, *Introduction to Polymers*, 3rd ed., CRC Press, Taylor and Francis Group: Boca Raton, 2011.
[29] Baskaran D, Müller A. *Prog. Polym. Sci.* 2007, 32, 173–219.
[30] Wilms D, Klos J, Frey H. *Macromol. Chem. Phys.* 2008, 209, 343–356.
[31] Wurm F, Wilms D, Klos J, Löwe H, Frey H. *Macromol. Chem. Phys.* 2008, 209, 1106–1114.
[32] Ziegenbalg D, Kompter C, Schönfeld F, Kralisch D. *Green Proc. Synth.* 2012, 1, 211–241.
[33] Nagaki A, Tomida Y, Yoshida J. *Macromol.* 2008, 17, 6322–6330.
[34] Iida K, Chastek TQ, Beers KL, Cavicchi KA, Chun J, Fasolka MJ. *Lab Chip* 2009, 9, 339–350.
[35] Engler M, Kockmann N, Kiefer T, Woias P. *Chem. Eng. J.* 2004, 101, 315–322.
[36] Gilman H, Gaj BJ. *J. Org. Chem.* 1957, 22, 1165–1168.
[37] Stanetty P, Koller H, Mihovilovic M. *J. Org. Chem.* 1992, 57, 6833–6837.
[38] McCrackin FH. *Polymer* 1987, 28, 1874–1850.
[39] Mello IL, Delpech MC, Coutinho FMB, Albino FFM. *J. Braz. Chem. Soc.* 2006, 17, 194–199.
[40] Hayduk W, Cheng SC. *Chem. Eng. Sci.* 1971, 26, 635–646.
[41] Chalykh AY, Titkova LV, Malkin AY, Dreval VY, Pronin IS. *Polym. Sci. USSR* 1974, 16, 2134–2144.

Simon Schulze studied chemistry at the University of Stuttgart. During his diploma thesis at the Institute of Chemical Technology in the group of Professor Weitkamp, he worked on heterogeneous catalysis and obtained his Dipl.-Chem. degree in 2009. In the same year, he joined the group of Professor Klemm, where he started his PhD thesis within the CoPIRIDE project of the FP7 program by the EU. Until now, he has worked on the process intensification of the anionic polymerization of 1,3-butadiene in a capillary reactor. Simon Schulze plans to graduate in 2013 (PhD degree).

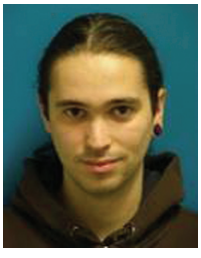

Bruno Cortese got both his Bachelor and Masters degrees in Industrial Chemistry at the Universita' degli studi di Milano (Italy), specializing in physical chemistry and catalysis. Since 2009, he has been enrolled as a PhD student of Chemical Engineering at the Eindhoven University of Technology, The Netherlands. His main research interests are numerical optimization and computational fluid dynamics applied to process intensification problems.

Matthias Rupp studied Chemical Engineering at the University of Karlsruhe. His diploma thesis dealt with the partial oxidation of o-xylene to phthalic anhydride under supervision of Professor B. Kraushaar-Czarnetzki. Currently he is working on his PhD thesis under Professor E. Klemm at the Institute of Chemical Technology at the University of Stuttgart, where he is investigating the kinetics of alcohol ethoxylations in microstructured reactors.

Mart de Croon is assistant professor in Chemical Engineering at TU/e. He received his PhD in Physical Chemistry at Radboud University, Nijmegen, in 1980, and was active at the same university in the areas of catalysis (1981–1985), electrochemistry (1985–1986), and solid state physics (1986–1990). In 1990 he joined the Faculty of Chemical Engineering and Chemistry in Eindhoven, to work on Chemical Vapour Deposition and on the kinetics of high temperature processes. His present research concerns micro reaction technology.

Volker Hessel studied chemistry at Mainz University and obtained his PhD in the field of organic chemistry in 1993. In 1994, Professor Dr. Hessel started his professional career at the Institut für Mikrotechnik Mainz GmbH (IMM). In 1999, he was appointed Head of the Microreaction Technology Department, and in 2007, he was appointed as Director R&D at IMM. In 2005, he followed a part-time appointment as professor for the chair of "Micro Process Engineering" at Eindhoven University of Technology, TU/e. In 2009, Volker Hessel was appointed as honorary professor at the Technical Chemistry Department at Technical University of Darmstadt. In 2011, he was appointed as full professor for the chair of "Micro Flow Chemistry and Process Technology" at the Eindhoven University of Technology, TU/e. Professor Dr. Hessel is author or co-author of more than 250 peer-reviewed publications, 18 book chapters, and five books. His current research covers the development of harsh chemistries (high-pressure, high-temperature, solvent-less) and the full process design and cost/LCA evaluation of smart-scaled flow processes, using microreactors or similar equipment. He received the AIChE award "Excellence in Process Development Research" in 2007. He received the ERC Advanced Grant for his research topic "Novel Process Windows" in 2010. He is Editor-in-Chief of *Green Processing and Synthesis*.

Since 2012, Julien Couet has worked for Evonik Industries managing investment projects (up to 8 Mio €). He received a double Master in Organic Chemistry at CPE Lyon (France) and Heriot-Watt University Edinburgh (Scotland). His academic education was completed with a PhD work in 2007 focusing on the modification of peptide structure by addition of polymer at the University of Freiburg (Germany). In 2008, he started his professional career at Evonik Industries, occupying several R&D Manager positions in the business units "Performance Polymers" and "Oil Additives" until 2012. His expertise concerns design and production of various polymers.

Jürgen Lang is Senior Scientist in the Innovation Management of the Process & Engineering department (TE). After education in computer technology at Messerschmitt-Bölkow-Blohm and studies in high and highest frequency technology at KIT – Karlsruhe Institute of Technology, Dr. Lang earned his doctorate in Plasma-Catalytic Effects in Ammonia Synthesis from KIT-Institute of Physical Electronics. After interdisciplinary scientific work from 1987 until 2000 at Fraunhofer Institut for System Technology and Innovation Research (FhG-ISI), he joined the New Process Department of former Degussa-Hüls in 2000. In 2010, he switched to the Innovation Management of the TE department.

Elias Klemm was appointed full professor of Heterogeneous Catalysis and Chemical Technology at the University of Stuttgart in 2009. Prior to that, he had been full professor of Chemical Technology at the University of Chemnitz for 5 years. He worked for 2 years as Process Engineer in the field of Chemical Micro Process Engineering at Degussa AG in Hanau. Elias Klemm studied chemical engineering at the University of Erlangen-Nuremberg and received his PhD in the field of heterogeneous catalysis in 1995.